Introduction of a Biologically Plausible Color Descriptor to a Neurodynamical Model of the Primary Visual Cortex

Sean Thomas Connolly

Abstract

We present a computational model of color description & processing in the primary visual cortex (V1), inspired by current neurobiological understanding. This understanding posits single and double-opponent neurons as fundamental to low level color processing. We offer a novel representation of color by defining these cells' responses and the connections between them, within the framework of a dynamical model of neuronal activity. Our model reproduces perceptual experiences in a number of cases, offering credence to said biological theories.

Index Terms

primary visual cortex, striate cortex, V1, receptive field, single-opponent, double-opponent, color assimilation, color induction

I. INTRODUCTION

COLOR induction and contrast are two related, opposing, perceptual phenomena. The former is a change in perceived color "toward" a nearby color, while the latter is a change of one color "away" from the nearby color. Neurophysiological research suggests that these phenomena may arise as early in primate vision as the primary visual cortex (V1). It is proposed that the boundaries between two colored regions drive these effects. Specifically, research in the field describes neurons which fire selectively to boundaries between certain colors, so called double-opponent cells, and identifies them as being critically related to the color perceived.

Within, we propose a computational model designed around the current understanding of this biology. We present two implementations, one more biologically accurate, and another more computationally elegant. We explore the behavior of these models with respect to what they can teach us about the assumed biological theories, as well as their application to the field of computer vision.

II. STATE OF THE ART

A. Neurobiology

Historically, it was widely believed that color and shape are two distinct aspects of visual perception. Truly, this line of thinking is intuitive: one can perceive the color of a flat surface which occupies our full field of vision, despite its lack of 'shape', likewise we can see the shape of achromatic objects, as in black and white film. This theory of perception innervated neurophysiological understanding. It was supported by neurobiological findings, such as that the lateral geniculate nucleus (LGN), the pathway which carries information from the retina to the primary visual cortex (V1), consists of three entirely distinct layers; two (the parvicellular and konicellular) carrying only color information, and one (the magnocellular) dealing purely in achromatic contrast (edge) information. Based on early anatomical observations, it was proposed that these three LGN pathways for color and contrast are then processed into two separate streams in V1, one for color and the other for form. This separate handling of color and form confirmed for researchers that, as suspected, these two perceptual concepts are processed separately in the brain.

Research in the past decade or so has seen a shift from this thinking, however. Psychophysical observations, such as those in Figure 10, influenced researchers to consider that color and form are more intrinsically related than previously thought. In these examples, we see that the perceived color of the inner square is highly dependent on the background and, most importantly, how the inner square *contacts* the background. That is to say, the color perceived is not just determined by the physical properties of the surface itself, but also by the context in which the surface is viewed. Furthermore, we can observe that this contextual influence comes largely from the boundary edges of the surface: in example (c), the dulling color assimilation effect witnessed in (b) is almost entirely negated by simply adding a thin border. That is, by removing contact between the inner square and the background the effect of the context is significantly reduced. In fact, "the color appearance of a region may be more dependent on color contrast at the boundary of the region than it is on the spectral reflectance of the region's interior." [11, p.572]

Author: Sean Thomas Connolly, connolly.st@gmail.com
Advisor: Xavier Otazu, Computer Vision Center, Computer Science Department, Universitat Autnoma de Barcelona, Barcelona, Spain
Submitted: September 2014

Fig. 1: Psychophysical example emphasizing the effect of edge contrast in color perception. In all cases, the center square is the same physical color. On (a) the green background, however, it appears much brighter than it does on (b) the red background. (c) Adding a thin black border negates the assimilation effect, increasing the perceived brightness of the center square. (d) Blurring the background, on the other hand, seems to enhance assimilation, lowering the perceived brightness at the center.
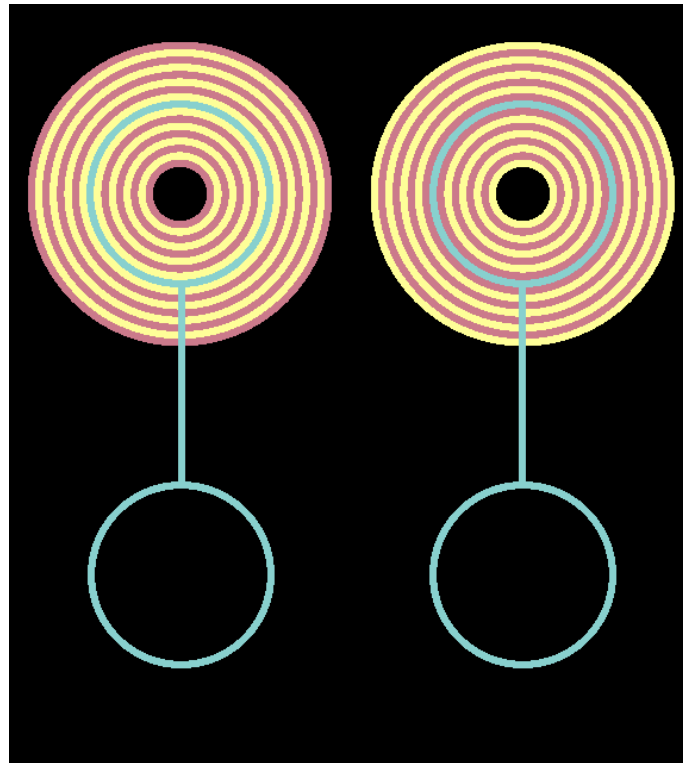

Fig. 2: Example of contextual influences on the perception of color. **//TODO** *DESCRIBE WHAT'S HAPPENING & THE IMPLICATIONS*

With these psychophysical observations in mind, much research has been devoted to elucidating the exact neurobiological mechanisms behind the perception of color, and the influence of form in it. The current view holds that while the LGN does indeed carry color and contrast information through separate pathways to V1, once there, color and form become deeply intertwined as they are processed further. To explain this influence of form on color processing in V1, the literature proposes two broad classifications of neurons: single-opponent cells & double-opponent cells [4].

Opponency, in neurobiology, refers to antagonistic inputs of information: one source of input excites the neuron, while another inhibits it. These two antagonistic components of opponency are commonly referred to as the *on* and *off* inputs to a neuron. One can think of these two inputs as being what the cell is 'looking for', *on*, and what the cell is 'not looking for', *off*. Intuitively, stimuli from the *on* input excites the neuron, while stimuli from the *off* input inhibits it. Perhaps less intuitively, removal of stimuli from the *off* input also excites the neuron. This behavior is logical when you consider that the two antagonistic inputs typically represent mutually exclusive features. In this way, removal of the negative stimuli often means much the same as presence of the positive stimuli and thus, removal of such stimuli contributes to excitation of the neuron. Of course, if equal stimuli are provided from both the *on* and *off* inputs, excitation is cancelled out by inhibition and the neuron does not fire. Lastly, recognize that any one neuron usually receives antagonistic input from, in fact, many other neurons. The aggregate stimuli from these excitatory and inhibitory inputs determines if the cell fires.

With respect to cells in the early visual system, we specifically use opponency to refer to chromatic and spatial opponency. We will now detail what exactly this means, with specific examples of neurons' expected patterns of response to various stimuli, as well as the implications of such responses. To frame this explanation, consider that single-opponent cells respond best to *large areas* of light/color, while double-opponent cells respond only to the *boundaries* between such areas.

Single-Opponent Neurons

Single-opponent cells are a class of neurons in the early visual system which respond best to large areas of color and/or luminance. Their behavior is achieved by constructing classical center-surround receptive fields. The center receptive field serves as the *on* input, exciting the cell when presented with a particular color, while the surround receptive field serves as the *off* input, inhibiting the cell when another color is present or exciting it when that color is removed. These center and surround receptive fields may involve very few retinal cones, or may span many degrees of vision [5].

In so called color preferring single-opponent cells, the cone inputs to the center and surround come from cones with different spectral response functions, e.g.: L vs M. By arranging input from different cones into antagonistic receptive fields, we get a neuron which is sensitive to a particular color, in opposition to another. In the human visual system, we recognize three axes of such color opponency: redness vs. greenness, blueness vs. yellowness, and lightness vs. darkness. To construct these concepts of color, neurons in the visual pathway contrast activity of the three types of cone cells: those sensitive to long (L) wavelength light, those sensitive to medium (M) wavelength light, and those sensitive to short (S) wavelength light. By contrasting relative activity with neighboring L, M, and S cones, the retina itself can already begin to construct signal resembling psychological concepts of 'color'.

//TODO *add image of simple behavior: gradient response to isoluminant chromatic boundary*
//TODO *add image of simple behavior: no response to intensity changes*
//TODO *add image of ON/OFF differences: R-G cell responds to fullscreen green light removed (not red removed)*
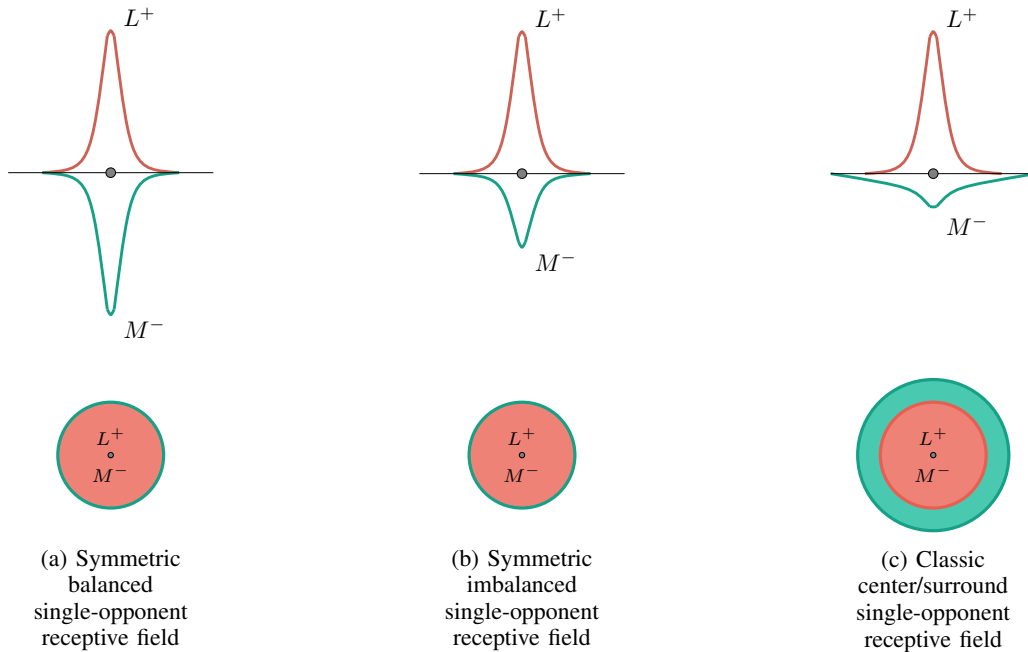
Fig. 3: Examples of possible single-opponent receptive field configurations, many others could be designed. All function to describe color properties of surfaces, though their response patterns to similar stimuli vary slightly.

(a) Symmetric balanced single-opponent receptive field

(b) Symmetric imbalanced single-opponent receptive field

(c) Classic center/surround single-opponent receptive field

As mentioned, one of the three axes of the opponent process theory is lightness vs. darkness. This is achieved in single-opponent cells by providing opponent inputs into the *on* center and the *off* surround from the same cones. By including input of L, M, and/or S cones into both the center and surround, the cells becomes 'color blind' and instead only respond to changes in luminosity. Sometimes incorrectly labeled as 'non-opponent', these neurons are, indeed, single-opponent cells: achromatic single-opponent cells.

//TODO *add image of simple behavior: gradient response to ((mono)chromatic) intensity changes*
//TODO *add image of simple behavior: no response to isoluminant chromatic boundaries*

Double-Opponent Neurons

We have defined single-opponent cells to best respond to large areas of light/color. We now define double-opponent cells to respond only to the boundaries between such areas. In this regard, it is fair to think of double-opponent cells as biological 'edge detectors'. However, the precise definition of these cells is a topic of confusion in the field of neurobiology. All involved seem to agree that the input to the neuron is that of two single-opponent neurons itself. In this sense, the term "double-opponent" can be thought of as indicating that the dimensionality of color opponency has been doubled. However, another camp of researchers take the definition a step further and suggest that the two SO inputs are spatially offset. By this definition, the term "double-opponent" is thought to indicate that the cell is sensitive to opponency in two *different* dimensions: color and space.

The distinction is non-trivial as the response patterns differ significantly, and thus the interpretation of their role in vision differs. Truly, both types of cells may, and likely do exist in the primate visual system [**//TODO** *Cite studies which find these cells*]. However, for the purpose of our work we only consider the latter definition: double-opponent cells' receptive fields are both chromatically and spatially antagonistic.

//TODO FIGURE: present the differences between the two DO configurations

(a) Symmetric balanced double-opponent receptive field

(b) Symmetric imbalanced double-opponent receptive field

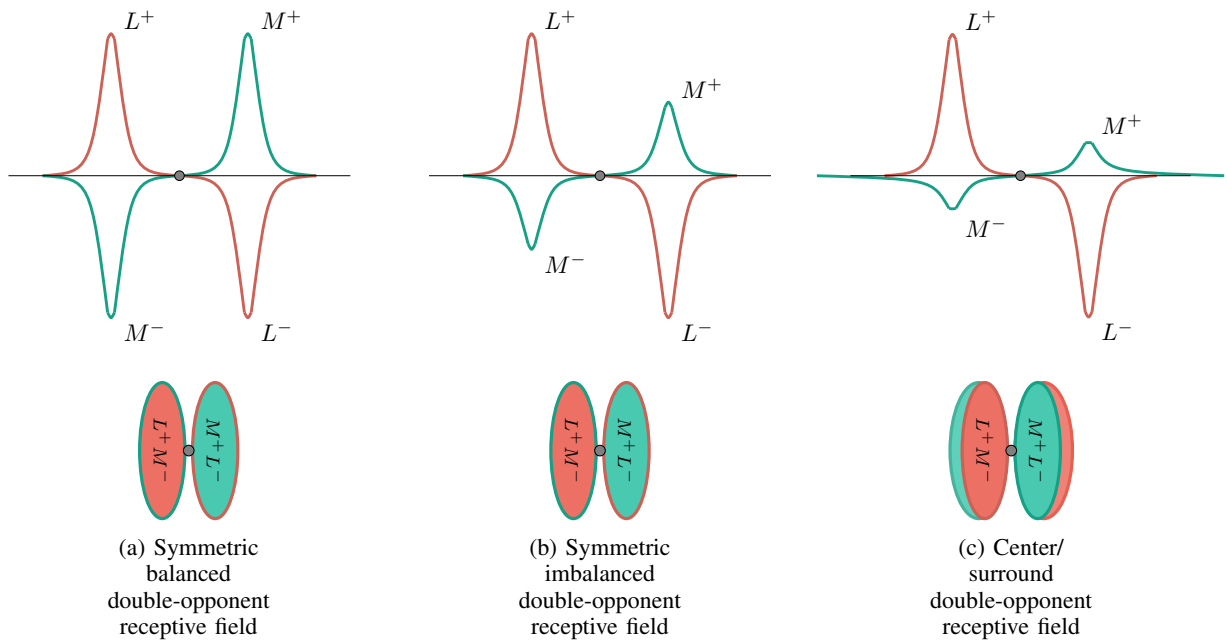(c) Center/ surround double-opponent receptive field

Fig. 4: Examples of various possible double-opponent receptive field configurations, many others could be designed. All function to describe color properties of borders, though their response patterns to similar stimuli vary slightly.

Orientation Selectivity: Research shows that cells identified as double-opponent tend to be orientation selective [4], [14], [12], [**?**]. That is, they respond most strongly when stimulated by a border of particular orientation, less so with variation from that preferred orientation, and weakly, if at all, to borders orthogonal to the preferred orientation. This is intuitive given the organization of the receptive field as previously defined. By arranging the components of the receptive field to be spatially antagonistic, there will be one orientation of border which best separates the two components, and another orientation, precisely orthogonal, which does not separate the two components at all. This can be easily visualized, as in Figure **??** and Figure **??**.

//TODO *add image of simple behavior: peak activity AT sharp edge*

It's worth noting that a single-opponent neuron can also be selective to specific orientations. These cells have been identified in biology, though their relative abundance appears minimal. To achieve orientation selectivity, the center and/or surround receptive fields simply need be made non-circular. However, without the balanced asymmetric *on* and *off* receptive fields from each opponent cone(s), an orientation specific single-opponent cell could never be as selective as a double-opponent cell.
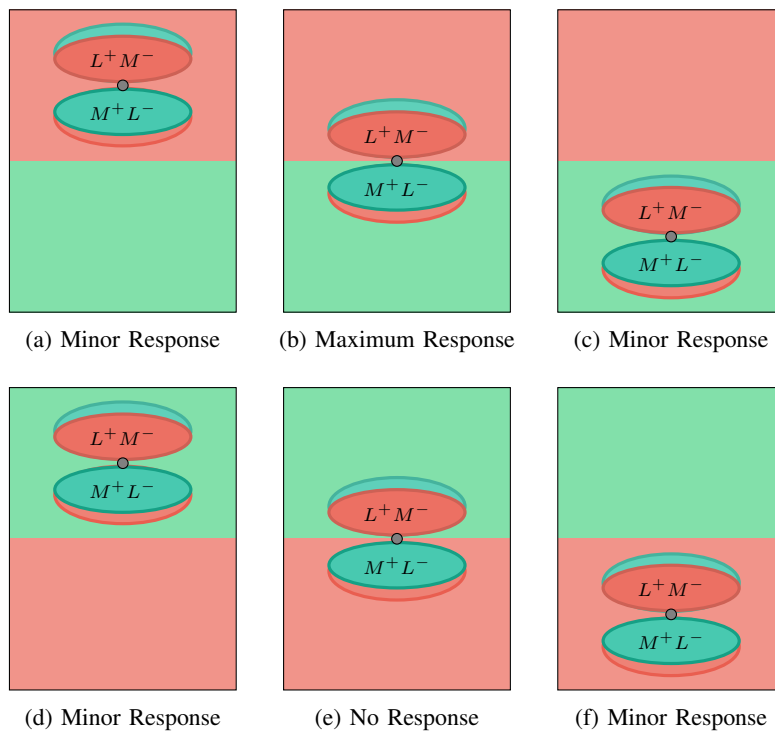
Fig. 5: A double opponent cell selective to horizontally oriented borders with red above and green below; only responsive to that particular stimulus. In Figure (b), the neuron is presented with its ideal stimulus: its L^+ and M^+ receptive fields are fully activated while its L^- and M^- receptive fields are completely unactivated. Figure (e) presents the neuron with the exact opposite stimulus, neither its L^+ nor M^+ receptive fields are activate at all, and both its L^- and M^- receptive fields are fully activated, ensuring no response possible from the cell. While its L^+ receptive field might be strongly stimulated in (a) and (f), it's L^- receptive field cancels it out. Similarly, in (c) and (d) its M^+ receptive field is stimulated but cancelled out by activity in its M^- receptive field.

(a) Minor Response   (b) Minimal Response   (c) Minor Response

(d) Minor Response   (e) Minimal Response   (f) Minor Response

Fig. 6: A double opponent cell selective to vertically oriented borders with red to the right and green on the left; completely unresponsive to a horizontal border. While its L^+ receptive field might be strongly stimulated in (a) and (f), it's L^- receptive field cancels it out. Similarly, in (c) and (d) its M^+ receptive field is stimulated but cancelled out by activity in its M^- receptive field. In (b) and (e) both of its L^+ and M^+ receptive fields are moderately activated, but again, cancelled out by activation in its L^- and M^- receptive fields, respectively.

Spatial Frequency Selectivity: Another important feature of double-opponent cells is that they are inherently sensitive to borders of specific size, or scale. Technically, we refer to such preference of 'scale' as a cell's spatial frequency selectivity. Each double-opponent neuron will be selective to a particular spatial frequency and excited less so by stimuli of spatial frequency deviating from this preference. Again, this is quite intuitively a product of the design of the neuron's receptive field and easily visualized, as in Figure 7.

(a) Maximum Response   (b) Maximum Response   (c) Maximum Response

Fig. 7: A double opponent cell tuned to a particular spatial frequency. Either a (b) lower or a (c) higher spatial frequency than preferred lowers the response of the cell.

//TODO *CONTRAST WITH SINGLE-OPPONENT'S LACK OF SPATIAL FREQ. SELECTIVITY (show Shapley's graphs) [erm.. don't we have spatial frequency for SO also??]*

Achromatic Double-Opponent Neurons: As with single-opponent cells, one of the axes of the opponent process theory is 'lightness' vs 'darkness'. While we frequently discuss opponency as being a thing of 'color', we find double-opponent cells which are specifically sensitive to luminance borders. Such achromatic sensitivity is easily achieved by balancing cone inputs into the neuron's antagonistic receptive fields, as in single-opponent cells. It behaves just as the previously described double-opponent cells, with specific orientation and spatial frequency selectivity, but responds best to luminosity borders rather than

chromatic borders. For more details on achromatic receptive fields, please refer back to the section on *Achromatic Single-Opponent Neurons*. It is important to reiterate here that the *on* and *off* inputs to light and dark sensitive single-opponent cells are balanced, whereas their chromatic sensitive counterparts are imbalanced in inputs (**//TODO** *incorrect terminology, we use 'imbalanced' differently in SO graphics*). This has the implication at the double-opponent level that light and dark double-opponent cells are redundant, as can be seen in Figures 11a and 11b. This is in contrast to the chromatic double-opponent cells depicted in Figure 11 which differentiate themselves from their opponent pair by imbalanced inputs from the same cones.

Hypercolumns

Thus far we have defined two broad classes of neurons in the primate visual system: single-opponent and double-opponent. Each class has a number of parameters which dictate what stimuli the cell should respond to: opponent color, orientation selectivity, and spatial frequency. A single cell can only be sensitive to a specific combination of settings for each parameter. However, for each parameter it is important to have neurons sensitive to the full range of parameters. Thus, it is necessary to have a collection of neurons which together cover the complete combinatorial set of settings for all parameters.

Furthermore, as may be obvious, the receptive field of a neuron in V1 is directly **connected/related/tied** *(???)* to a set of neurons in the retina. That is, neurons in V1 are sensitive only to activity at a particular physical location on the retina; V1 is *retinotopic*, or retinally mapped.

The implication is that for each retinal position, in V1 it is necessary to have a large number of both single-opponent and double-opponent cells, selective to the full gamut of parameters possible for each type of cell. Biologically, these collections of cells are organized in *hypercolumns*, a physical grouping of cells in which neuronal connections 'up' and 'down' within the column are much more dense than extensions to cells in other columns. Within a single hypercolumn, all cells are sensitive to a specific retinal location, but together express sensitivity to the full range of parameters.

//TODO *mention relative abundance of SO, & DO*
//TODO *add image of Shapley response curves for SO, & DO*

CO Blobs
//TODO *PARAGRAPH ON WHERE DO CELLS ARE*
//TODO *PARAGRAPH ON WHERE SO CELLS ARE*
//TODO *PARAGRAPH ON PROPOSED CONNECTIONS BETWEEN DO & SO*

B. Computational Modeling:

The model described in this research is an extension of that presented by Penacchio *et al.* [**?**], itself based on work by Z. Li [6], [7]. Before detailing our implementation, it is important to review prior art; these works and others. As our goal is to model the behavior of color preferring and achromatic single-opponent and double-opponent neurons, we will also review other computational endeavors tackling the issue of color and/or form from a biologically inspired perspective.

Li's Neurodynamical Model for Segmentation (1999)

In Li's original work, a neurodynamical model was presented which focused on global region segmentation using only local interactions between neurons. In the interest of simplicity, Li's implementation dealt only with the nature of these interactions, ignoring where the stimulus, or information, might be coming from. Conceptually, Li defined neurons by their physical position in the image and the 'feature' to which they are sensitive. She then defined the connections between these neurons such that those physically close to each other, and sensitive to similar features, interacted most strongly. Stimulation of one neuron, then, positively stimulated (excited) similar neurons nearby, and negatively stimulated (inhibited) dissimilar neurons nearby. Such excitation and inhibition cascades through the network naturally, producing large scale response patterns defined only by local stimuli.

In the model presented, Li used oriented bars as features, though expressed that any logical feature could be reasonably considered in its place. This choice was biologically inspired by neurons sensitive to specifically oriented bars, the afore-mentioned double-opponent cells. When considering such features, inter-neuronal connections can be logically deduced: two neurons positively interact most when both 1) are sensitive to similarly oriented bars and 2) are co-located along that same orientation. Two neurons negatively interact most when either of these two conditions is not met.

//TODO *include graphic or oriented bars which positively & negatively interact*

By defining neuronal connectivity in this manner, patterns of neurons sensitive to co-located and co-aligned bars positively interact with each other to enhance their collective response to the stimuli. Similarly, incoherent stimuli negatively interact with their neighbors and are silenced. From these local interactions, global features are enhanced if they satisfy the connectivity rules, and noise is suppressed. Li showed that this method can be used to enhance contours and identify boundaries between regions for which normal segmentation methods struggle.

Penacchio, Otazu, & Dempere-Marco's Neurodynamical Model for Brightness Induction (2013)

Li's work laid the foundation for Penacchio *et al.* who extended the model to a usable framework which:

1) Uses real black & white images /movies as input.
2) Utilizes discrete wavelet transforms to extract edges (more on this later).
3) Added multi scale support.
4) Summarizes the results into an output 'perceptual image'.

Their research was focused on observing brightness induction (BI) arising from such a neurodynamical model.

- No color, just black & white *edges*
- Generalized to real images (edges vs lines)
- Added scales
- Dynamical processing
- **Avoid detail, save that for *Method*..?**
- Extension of Z. Li's edge detection work
- Uses DWT to extract oriented edges in grayscale
  - ..in our context, it's essentially a luminance sensitive double-opponent cell.

Itti, Koch, & Niebur's Model for Saliency [3]

Itti *et al.* implemented a biologically inspired model of visual attention, or saliency. This work included opponent processing of color, center/surround receptive fields at scales, and orientation selectivity. Because of these features, and their overlap with our own goals, we consider it an important work to consider.

Color is included in this model by treating the color channels of the RGB image as analogous for L, M, and S cone activity. From this, red, green, blue, and yellow color components, as well as a single intensity components are derived, using the following formulae:

$$I = \frac{(r + g + b)}{3} \tag{1}$$

$$R = max(0, r - \frac{(g + b)}{2}) \tag{2}$$

$$G = max(0, g - \frac{(r + b)}{2}) \tag{3}$$

$$B = max(0, b - \frac{(r + g)}{2}) \tag{4}$$

$$Y = max(0, \frac{(r + g)}{2} - \frac{|(r + g)|}{2} - b) \tag{5}$$

Each of the r, g, and b channels are normalized by I in order to decouple hue from intensity.

These derived color components (and intensity) are computed for a set of images convolved in a *Gaussian pyramid* and contrasted across scales to obtain center/surround opponent color (and intensity) channels:

$$I(c, s) = |I(c) \ominus I(s)| \tag{6}$$

$$RG(c, s) = |(R(c) - I(s)) \ominus (G(s) - R(s))| \tag{7}$$

$$BY(c, s) = |(B(c) - Y(s)) \ominus (Y(s) - B(s))| \tag{8}$$

Itti *et al.* also compute orientation features by deconvolving I with oriented *Gabor pyramids* at scale ($O(\sigma, \theta)$). These responses are then contrasted across scales to obtain orientation feature maps ($O(c, s, \theta)$):

$$O(c, s, \theta) = |O(c, \theta) \ominus O(s, \theta)| \tag{9}$$

Biologically, such features could be considered representative of achromatic double-opponent cells. Similar to the features obtained by Penacchio *et al.* use of discrete wavelet transforms (DWT), they include information about the intensity, position, and orientation of edges.

This set of 42 feature maps; intensity at 6 scales, 2 opponent colors at 6 scales each, and 4 orientations at 6 scales each, provide input for a dynamical neural network. In their neurodynamical model of saliency, each point of the feature maps represents activity of a neuron and interactions between neurons ensure that only the most active locations remain, while all others are suppressed.

//TODO *Review significance of this work on ours (why do we care?)*

Yang, Gao, Li & Li's Model of Boundary Detection [?]

Yang *et al.* developed a biologically inspired system of edge detection. To this end, they implemented a model of chromatic double-opponent receptive fields constructed from asymmetric gaussian filters. The first step in their algorithm is to transform the RGB input image to red, green, blue, and yellow opponent color channels. Their approach simply utilizes the red, green, and blue color channels as they are, and define yellow to be the average of red and green input.

$$R = r \tag{10}$$
$$G = g \tag{11}$$
$$B = b \tag{12}$$
$$Y = \frac{r + g}{2} \tag{13}$$

These four color components are then convolved with centered, circular gaussian filters. This can be interpreted as modeling the receptive fields of chromatic single-opponent cells. These single-opponent cell responses are then combined in spatially opponent pairs to derive models of chromatic double-opponent cells.

//TODO *DESCRIBE THEIR USE OF SCALE (GAUSSIAN σ)*

//TODO *DESCRIBE THEIR HANDLING OF ORIENTATION (abs, max, mean?)*

For their purposes of boundary detection, they evaluate their modeling of double-opponent cells only, discarding single-opponent cell responses. However, their implementation of single-opponent cells is perfectly reasonable and taken as inspiration in our work. The primary shortcoming of the research by Zhang *et al.* lies in the description of color itself; while convenient, it is not supported by biology thus needs to be rethought.

Zhang, Barhomi, & Serre's Biologically Inspired Color Descriptor [?]

Zhang *et al.* introduce a computational color descriptor which integrates color and form. They specifically aim to model the behavior of single-opponent and double-opponent cells in the primate visual system. To do so, they consider the three classical opponent axes (Red-Green, Blue-Yellow, Light-Dark), as well as a fourth (Red-Cyan), omitted here.

Single-opponent cells' responses are modeled by first convolving the RGB input with a center (c) surround (s) filters, and then applying the following transformations:

$$R(c, s) = \tfrac{1}{\sqrt{2}} r(c) + \tfrac{-1}{\sqrt{2}} g(s) \tag{14}$$
$$G(c, s) = \tfrac{-1}{\sqrt{2}} r(s) + \tfrac{1}{\sqrt{2}} g(c) \tag{15}$$
$$B(c, s) = \tfrac{2}{\sqrt{6}} b(c) + \tfrac{-1}{\sqrt{6}} r(s) + \tfrac{-1}{\sqrt{6}} g(s) \tag{16}$$
$$Y(c, s) = \tfrac{1}{\sqrt{6}} r(c) + \tfrac{1}{\sqrt{6}} g(c) + \tfrac{-2}{\sqrt{6}} b(s) \tag{17}$$
$$L(c, s) = \tfrac{1}{\sqrt{3}} r(c) + \tfrac{1}{\sqrt{3}} g(c) + \tfrac{-1}{\sqrt{3}} b(s) \tag{18}$$
$$D(c, s) = \tfrac{1}{\sqrt{3}} b(c) + \tfrac{-1}{\sqrt{3}} r(s) + \tfrac{-1}{\sqrt{3}} g(s) \tag{19}$$

In this work the team explored three means of modeling single-opponent centers and surrounds: gradient operator, Gabor filters, and Gaussian derivatives. It is important to note that each of these models of receptive fields were oriented, and thus the models of single-opponent neurons presenter were, at least weakly, oriented themselves

//TODO *Mention half-squaring ($Inorm$?)*

To model double-opponent cell responses, single-opponent cell responses are further convolved with a number of oriented filters. These convolutions are then summed over phase and opponent pairs to yield three spatially and chromatically opponent channels; L-D, R-G, and B-Y (as well as R-Cyan in their work).

The output of their model is a set of feature maps representing the response patterns of single-opponent and double-opponent neurons selective to specific orientations.

//TODO *Review significance of this work on ours (why do we care?)*

Spitzer & Barkan's Model of Color Induction [16]

Spitzer *et al.* implemented a computational model of color induction by processing center and surround receptive fields of single and double-opponent neurons. While we also aim to model color induction, as well as brightness induction, our approach differs significantly from theirs. Our model seeks to introduce induction effects primarily through its neurodynamical

component, while theirs relies mostly on center and surround (and remote) effects introduced by the cells' receptive fields, as well as a temporal adaptation function.

Another important difference is that their implementation considered double-opponent cells to be circular concentric. That is, they accepted the definition of double-opponent cells which we discarded in our research (see *Double-Opponent Neurons* above). Using this definition of double-opponent cells, Spitzer *et al.* were able to model well chromatic induction and simultaneous contrast effects, though their model was not sensitive to oriented edges.

//TODO *REFERENCE DIAGRAM OF RECEPTIVE FIELD DIFFERENCE*

In their model they defined four opponent color components; red, green, blue, and yellow:

$$R(c,s) = r(c) - g(s) \tag{20}$$

$$G(c,s) = g(c) - r(s) \tag{21}$$

$$B(c,s) = b(c) - \frac{r(s) - g(s)}{2} \tag{22}$$

$$Y(c,s) = \frac{r(c) - g(c)}{2} - b(s) \tag{23}$$

This definition of the opponent color process seems, to us, more biologically plausible than those presented by Itti *et al.* [3], Yang *et al.* [**?**], or Zhang *et al.* [**?**]. Thusly, it will form the basis for our opponent color transformation, presented in the *Method* section below.

//TODO *MORE DETAIL?*

Comparison of Models

Our current work is a direct continuation of the research presented in the first two of these computational models. The latter four represent but a small selection of the wealth of effort being put into computationally describing color in a biologically plausible manner. It is important to recognize that these five models each had different specific research goals and so do not intend to be directly compared to one another. We present them here to frame our current work. Table **??** presents the features implemented in these models with respect to the goals of our work. This comparison elucidates our intentions: to bring biologically inspired descriptions of color to the neurodynamical processing model developed by Penacchio [9] and Li [7].

TABLE I: Comparison of computational models relevant to our current work.

	Proposed Model	Penacchio [9]	Li [7]	Itti [3]	Spitzer [16]	Yang [**?**]	Zhang [**?**]
Dynamical	Y	Y	Y	Y	Y	N	N
Intensity	Y	Y	N	Y	N	N	Y
Colors	Y	N	N	Y	Y	Y	Y
Scales	Y	Y	N	Y	N	Y	N
Orientations	Y	Y	Y	Y	N	Y	N
SO	Y	N	N	Y	Y	Y	Y
DO	Y	Y (achromatic)	N	Y	Y (concentric)	Y	Y
SO RF	Gaussian / DWT	N/A	N/A	Gaussian Pyramid	Gaussian	Gaussian	Difference of Gaussians
DO RF	Gabor-like Gaussians / DWT	DWT	N/A	Gabor Pyramid	Gabor	Gabor-like Gaussians	Difference of Gaussians
Goal	Color Induction	Brightness Induction	Saliency	Saliency	Color Induction	Edge Detection	Color Descriptor

Definition of criteria:

Dynamical:	Does the work attempt to model neurodynamical processes?
Intensity:	Does the work consider achromatic differences as features?
Colors:	Does the work consider chromatic differences as features?
Scales:	Does the work separate information at different scales?
Orientations:	If incorporating edge/boundary features, does the work distinguish between orientations?
SO:	Does the work attempt to model single-opponent cell behavior, directly or indirectly?
DO:	Does the work attempt to model double-opponent cell behavior, directly or indirectly?
SO RF:	If modeling single-opponent cells, how are their receptive fields defined?
DO RF:	If modeling double-opponent cells, how are their receptive fields defined?
Goal:	Generally speaking, what was the purpose of the modeling effort?

C. Summary

We define single-opponent neurons to possess classical center/surround receptive fields for processing cone input into opponent colors. We define double-opponent neurons to be spatially opposed combinations of single-opponent neurons. We recognize both achromatic and chromatic flavors of these cells, explaining the three axes of the opponent colorspace. By these definitions, we expect single-opponent neurons to respond best to fill field stimulation while double-opponent neurons fire only

at boundaries. This understanding treats color and shape as intrinsically connected and, as a consequence, predicts perceptual phenomena such as color induction to arise very early in visual processing.

The purpose of this project is to feed opponent color information into a neurodynamical model sensitive to edges and surfaces in a biologically inspired manner. The neurodynamical presented within is an extension of work done by Penacchio *et al.* [9] and Li [7]. To incorporate color into this model, we consider some of the previous work of biologically inspired color description. We find prior art to observe encouraging results when modeling the receptive fields of single and/or double-opponent neurons.

III. METHOD

We present a computational model designed to be representative of the aforementioned biology. The implementation of this model can be conceived of as two distinct parts:

- *Description of Visual Information:* transformation of image(s) into a biologically meaningful representation.
- *Neurodynamical Processing:* iterative processing of the dynamic interactions between the neurons modeled.
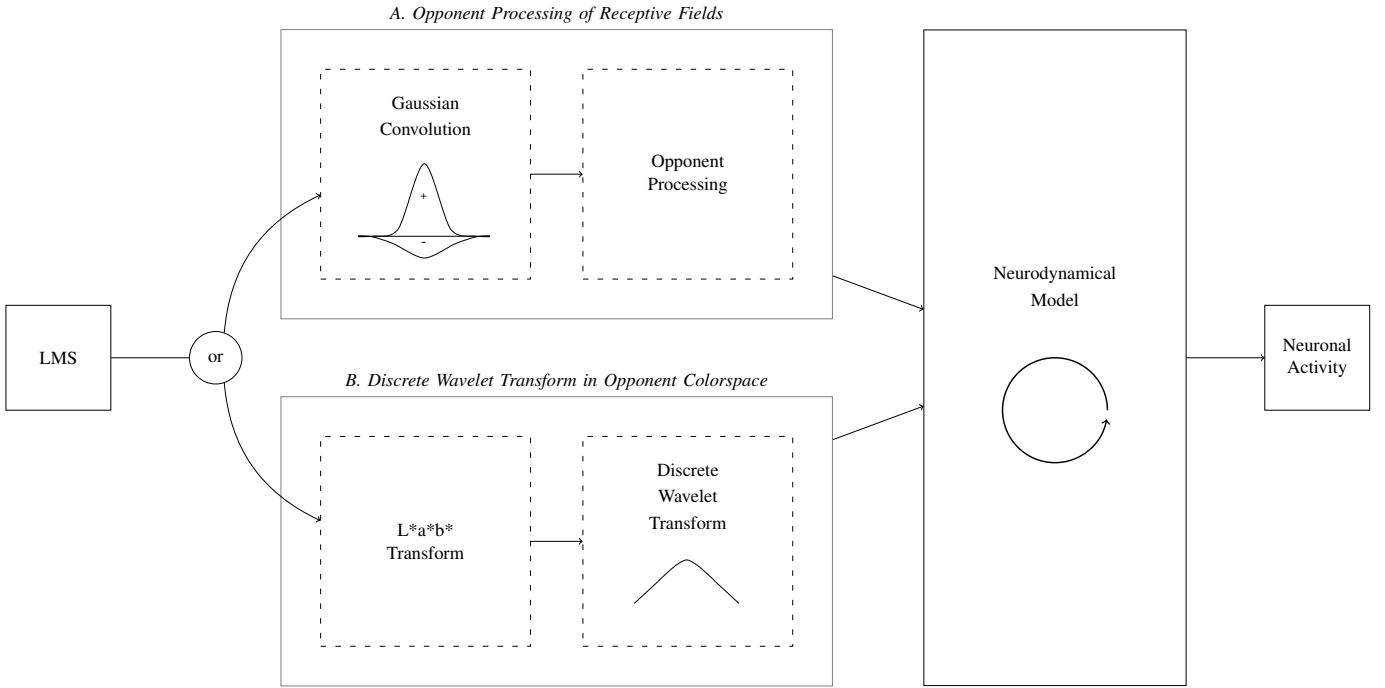

Fig. 8: Workflow diagram of algorithm at its highest level. Data can be processed through either *A. Opponent Processing of Receptive Fields* or *Discrete Wavelet Transform in Opponent Colorspace*. This is then fed into the neurodynamical model which outputs a map of neuronal activity.

Description of Visual Information

The opponent-process theory defines three axes visual information, obtained by processing of cone activity from the retina. These axes are Red-Green (R-G), Blue-Yellow (B-Y), and Light-Dark (L-D). Neurobiological research corroborates such processing of color information (**//TODO** *cite this*). **//TODO** *MORE ON OPPONENT-PROCESS THEORY*

//TODO *PARAGRAPH ON SINGLE AND DOUBLE OPPONENT CELLS*

In accordance with this understanding of biology, the image transformation process should 1) separate opponent color components from each other, and 2) separate surface information from boundary information. We describe two different approaches to this end. The first approach, herein referred to in prolixity as the "*Opponent Processing of Neural Receptive Fields*", represents an effort to explicitly transform raw visual data in strict accordance with neurobiological theory. Essentially attempting to mimic the information processing pathways of the retina, lateral geniculate nucleus (LGN), and striate cortex (V1). The second approach, termed with equal verbosity, is the "*Discrete Wavelet Transform in Opponent Colorspace*". Here we stray from the details of the biological pathways in an attempt to achieve the same end, through more computationally efficient means.

In both, the input is a normal RGB image, and the output to the neurodynamical model is a 5 dimensional matrix containing 6 opponent color channels (red (R), green (G), blue (B), yellow (Y), light (L), & dark (D)), each decomposed into its surface and oriented edge components, at 1 or more scales. In this work we consider just 3 directions of orientation preference at edges: horizontal, diagonal, & vertical. Before processing by the neurodynamical model, this data is normalized so as to circumvent

differences between the data output by these two methods. This normalization step is described in more detail in the section on *Neurodynamical Processing*.

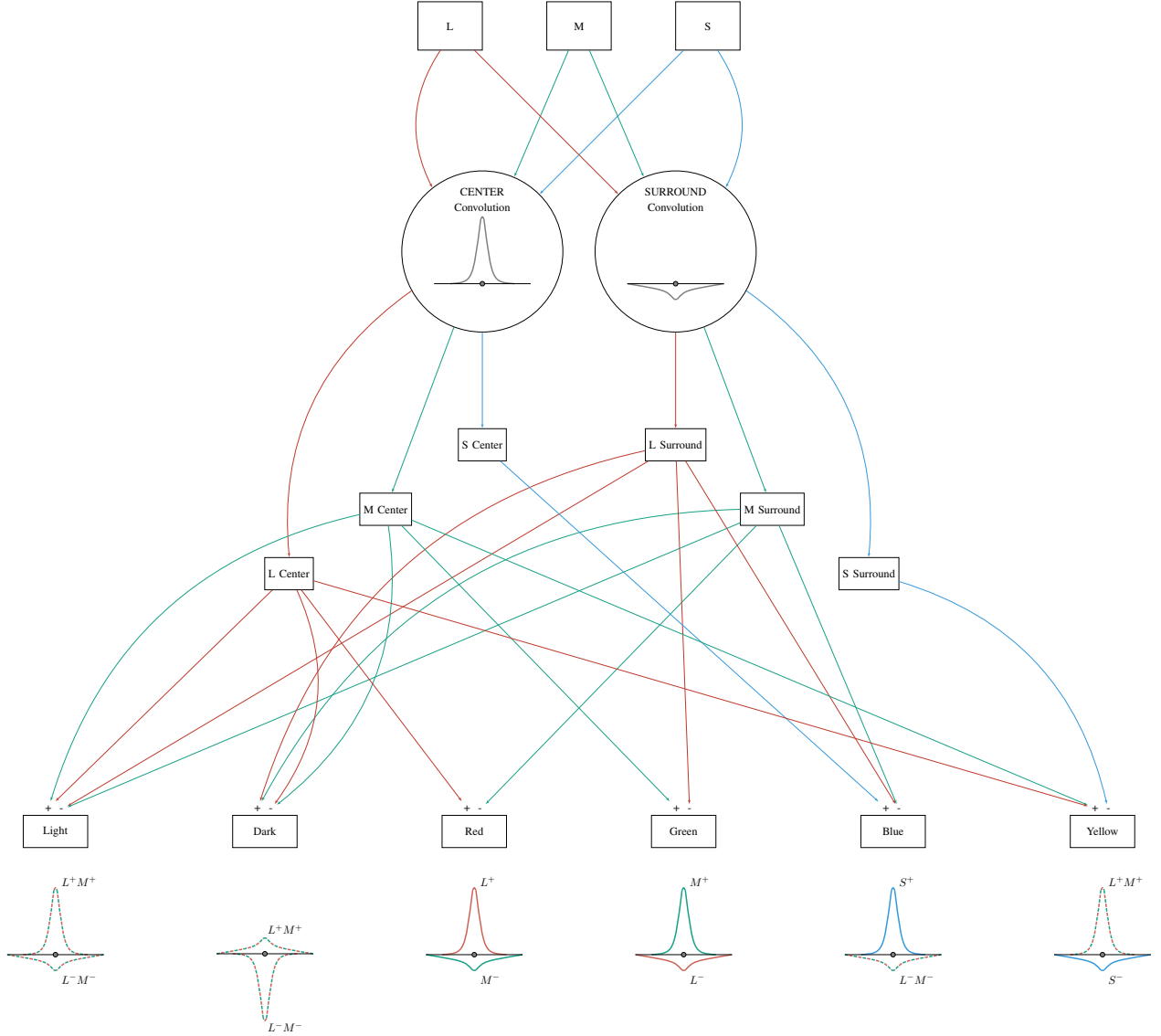## A. Opponent Processing of Neural Receptive Fields

Fig. 9: Diagram of *Opponent Processing of Receptive Fields* workflow. The L, M, and S channels are convolved with center and surround gaussians and then combined to build opponent colors, here exemplified by single-opponent cell receptive fields. The process is similar for double-opponent cells.

Neural Receptive Fields: **//TODO** *REFACTOR INTO PARAGRAPH ON RECEPTIVE FIELDS*
Opponent Processing: **//TODO** *REFACTOR INTO PARAGRAPH ON OPPONENT PROCESSING*

Processing starts by convolving each of the L, M, and S cone spectral response functions with two different gaussian filters. These convolutions simulate integration of information in a neuron's receptive field. One convolution is used to build the excitatory component of the receptive field (referred to as the center), the other convolution, the inhibitory (referred to as the surround).

Single-opponent cells' receptive fields are the classical center-surround configuration: symmetric, centered, circular gaussians. Typically, the center is smaller and weighed significantly more heavily than the surround, as in Figure **??** (c). Double-opponent receptive fields are markedly more complex: asymmetrical, off-center, elongated gaussian filters. Similarly, these filters can be adjusted to different sizes, shapes, and weights. For our tests we worked with symmetric balanced receptive fields, as in Figure **??** (a).

(a) Original

(b) Light Single-Opponent

(c) Dark Single-Opponent

(d) Red Single-Opponent

(e) Green Single-Opponent

(f) Blue Single-Opponent

(g) Yellow Single-Opponent

(h) Light Horizontal Double-Opponent

(i) Dark Horizontal Double-Opponent

(j) Red Horizontal Double-Opponent

(k) Green Horizontal Double-Opponent

(l) Blue Horizontal Double-Opponent

(m) Yellow Vertical Double-Opponent

(n) Light Diagonal Double-Opponent

(o) Dark Diagonal Double-Opponent

(p) Red Diagonal Double-Opponent

(q) Green Diagonal Double-Opponent

(r) Blue Diagonal Double-Opponent

(s) Yellow Diagonal Double-Opponent

(t) Light Vertical Double-Opponent

(u) Dark Vertical Double-Opponent

(v) Red Vertical Double-Opponent

(w) Green Vertical Double-Opponent

(x) Blue Vertical Double-Opponent

(y) Yellow Vertical Double-Opponent

Fig. 10: Example of single-opponent and double-opponent response (scale=1) to a test image following the *Opponent Processing of Receptive Fields* workflow. Strong activity is indicated by black and weak activity by white.

In our implementation, for convenience, we utilize the R, G, and B channels of the raw image as an approximation of L, M, and S cone activity, respectively. It should be noted that a preprocessing step could be performed to better match RGB to LMS so as to be more biologically consistent. The impact is likely negligible.

To construct opponent color channels, we contrast center (c) and surround (s) convolutions of the L, M, and S channels into three pairs: two color [16] and one achromatic.

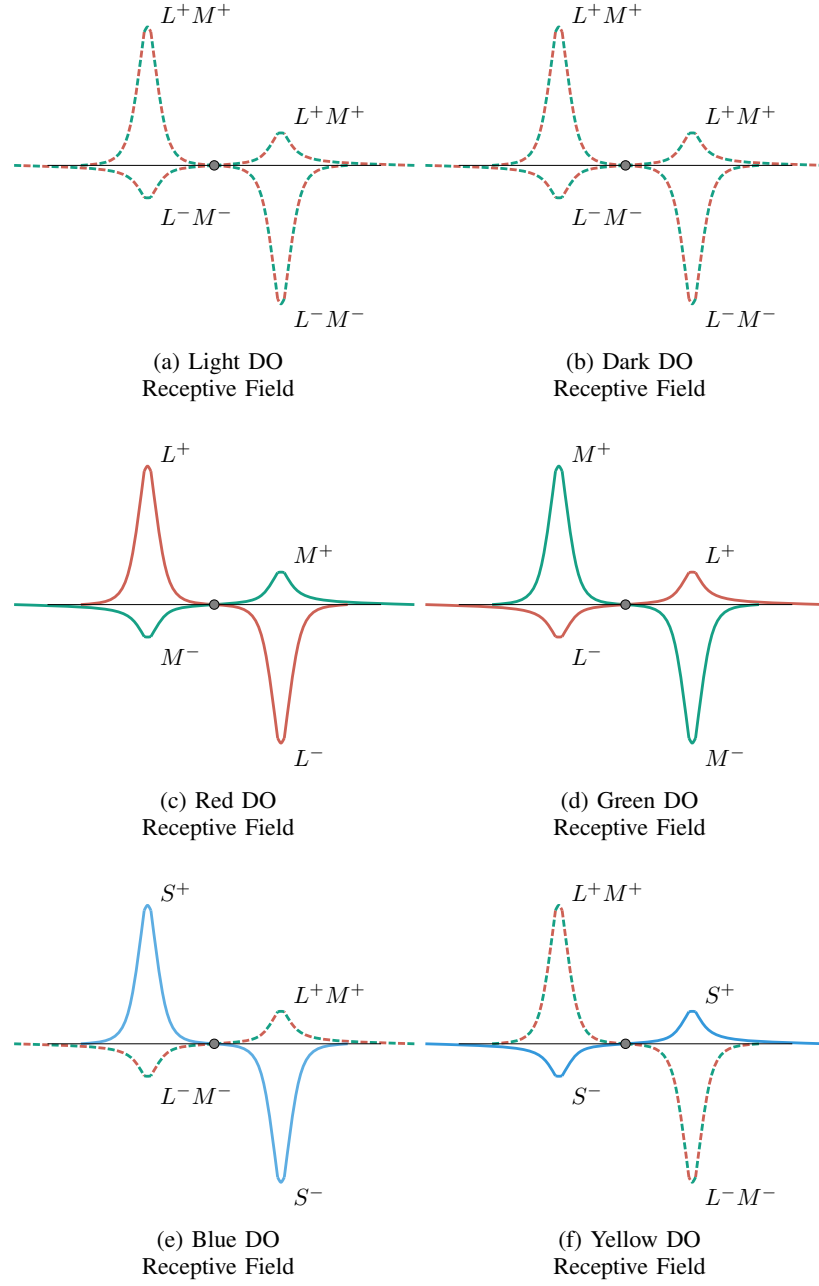(a) Light DO
Receptive Field

(b) Dark DO
Receptive Field

(c) Red DO
Receptive Field

(d) Green DO
Receptive Field

(e) Blue DO
Receptive Field

(f) Yellow DO
Receptive Field

Fig. 11

$$L(c,s,\sigma) = max(0,(\frac{L(c,\sigma)+M(c,\sigma)}{2}-0.5)-(\frac{L(s,\sigma)+M(s,\sigma)}{2}-0.5)) \qquad (24)$$

$$D(c,s,\sigma) = max(0,(\frac{L(s,\sigma)+M(s,\sigma)}{2}-0.5)-(\frac{L(c,\sigma)+M(c,\sigma)}{2}-0.5)) \qquad (25)$$

$$R(c,s,\sigma) = max(0,L(c,\sigma)-M(s,\sigma)) \qquad (26)$$

$$G(c,s,\sigma) = max(0,M(c,\sigma)-L(s,\sigma)) \qquad (27)$$

$$B(c,s,\sigma) = max(0,S(c,\sigma)-\frac{L(s,\sigma)+M(s,\sigma)}{2}) \qquad (28)$$

$$Y(c,s,\sigma) = max(0,\frac{L(c,\sigma)+M(c,\sigma)}{2}-S(s,\sigma)) \qquad (29)$$

//**TODO** *PARAGRAPH ON DOUBLE-OPPONENT ORIENTATIONS*

//TODO *PARAGRAPH ON SCALE*

1) Considerations:
- CON: Relatively slow
  - Could be improved with Gabor instead of gaussian for DO cells.
  - Could be improved by reusing SO info -¿ more biological
  - It's just an upfront cost, the neurodynamical processing is the most expensive.
- PRO: more receptive field control (explicit RF definitions)
- CON: requires tweaking of receptive fields
- PRO: more true to biology (combination of signal rather than numeric transformation of colorspace)
- CON: requires decision on meaningful RGB combination (should be elucidated from biology)
  - Pre-transformation to LMS might be valuable/meaningful.

Summary

This first of two approaches to color representation aims to be true to the biology at all cost. We explicitly model the receptive fields of both single-opponent and double-opponent neurons. These receptive fields are used to transduce retinal activity of L, M, and S cones into the cell activity expected in V1.

B. Discrete Wavelet Transform in Opponent Colorspace

Previous work by Penacchio *et al.* [**?**] utilized a discrete wavelet transform (DWT) to decompose a greyscale image into its oriented edge components, at scales. In the context of our current research, this could be thought of as representing achromatic double-opponent cells; the response is greatest at luminosity boundaries, and nonexistent on surfaces or at chromatic changes. In this work we extend their approach to the opponent colorspace and examine its applicability as a replacement of the previously detailed *Opponent Processing of Neural Receptive Fields*.

Opponent Colorspace: This transformation begins, not with the convolution step, but instead with a colorspace transformation. We convert the image from RGB to *CIE $L^*a^*b^*$*. This colorspace separates luminance from it's two opponent color channels. The two color channels are 0 centered, with both positive and negative values possible. The luminance channel, L^*, scales from 0 to 100, 0 being total darkness, 100 being pure brightness. We subtract 50 from this channel to obtain a 0 centered range of luminance. We consider positive values to define 'lightness' and negative values 'darkness'. From the opponent color channels, we take positive values in the a^* channel as denoting 'redness' and negative values 'greenness', while positive values in the b^* channel indicate 'blueness' and negative values 'yellowness'.

Discrete Wavelet Transform: Similar to the aforementioned use of gaussian filters, the application of the DWT can be interpreted as representative of the processing in a cell's receptive field. That is, the activity of a particular cell is defined not just by its own activity, but also of the activity of the cells around it. The key difference here being that the DWT is applied *in* the opponent colorspace, while in our previous approach the convolutions are applied to the raw L, M, and S input, before deriving opponent colors.

As all color channels are 0 centered, we can easily split them into independent opponent components:

$$Li_{do} = max(0, DWT(L^* - 50)) \tag{30}$$
$$Li_{so} = max(0, DWT(L^* - 50)_{residual}) \tag{31}$$
$$Da_{do} = |min(0, DWT(L^* - 50))| \tag{32}$$
$$Da_{so} = |min(0, DWT(L^* - 50)_{residual})| \tag{33}$$
$$R_{do} = max(0, DWT(a^*)) \tag{34}$$
$$R_{so} = max(0, DWT(a^*)_{residual}) \tag{35}$$
$$G_{do} = |min(0, DWT(a^*))| \tag{36}$$
$$G_{so} = |min(0, DWT(a^*)_{residual})| \tag{37}$$
$$B_{do} = max(0, DWT(b^*)) \tag{38}$$
$$B_{so} = max(0, DWT(b^*)_{residual}) \tag{39}$$
$$Y_{do} = |min(0, DWT(b^*))| \tag{40}$$
$$Y_{so} = |min(0, DWT(b^*)_{residual})| \tag{41}$$

//TODO *FIGURE: show diagram of oriented DWT filter (use TikZ)*
//TODO *FIGURE: show original & decomposed image*

//TODO *PARAGRAPH ON INTERPRETATION OF COMPONENTS (DO & SO)*
//TODO *PARAGRAPH ON WORKFLOW: RGB → L*a*b* (-50) → DWT → ON/OFF*
//TODO *PARAGRAPH ON PROS/CONS*

Neurodynamical Processing

Stage I of the proposed method focuses on the description of color in a biologically meaningful form, of which we've described two distinct approaches. Stage II is to further process this data in an iterative computational model of neurodynamical processes, as defined in Equations 42 and 43. The input stimulus, from Stage I, at time τ, $I_{i\gamma\sigma\theta}^{\tau}$ drives the model and mainly determines its response. The normalization of the stimulus at each time step is extended from that proposed by Li [7] and Penacchio [9]. We normalize within each color channel (γ), scale (σ), and orientation (θ). At the first time step, $I_{i\gamma\sigma\theta}^{1}$ is used to bootstrap the model and set as the initial excitation response, $x_{i\gamma\sigma\theta}$.

$x_{i\gamma\sigma\theta}$ can be viewed as a model of retinotopic excitation hypercolumns in V1, with i specifying the retinally mapped location of the hypercolumn. Similarly, $y_{i\gamma\sigma\theta}$ may be interpreted as its retinotopic inhibitory counterpart. $\dot{x}_{i\gamma\sigma\theta}$ and $\dot{y}_{i\gamma\sigma\theta}$, then, are the change in excitatory and inhibitory membrane potentials over time, respectively, and follow the equations:

$$
\begin{aligned}
\dot{x}_{i\gamma\sigma\theta} = & -\alpha_x x_{i\gamma\sigma\theta} \\
& - g_y(y_{i\gamma\sigma\theta}) \\
& - \sum_{\gamma' \neq \mathrm{opp}(\gamma), \Delta_\sigma, \Delta_\theta \neq 0} \Psi(\gamma', \Delta_\sigma, \Delta_\theta) g_y(y_{i\gamma\sigma+\Delta_\sigma\theta+\Delta_\theta}) + J_0 g_x(x_{i\gamma\sigma\theta}) \\
& + \sum_{j \neq i, \gamma' \neq \mathrm{opp}(\gamma), \sigma'\theta'} J_{[i\gamma\sigma\theta, j\gamma'\sigma'\theta']} g_x(x_{j\gamma'\sigma'\theta'})) \\
& + I_{i\gamma\sigma\theta}^{\tau} \\
& + I_0
\end{aligned}
\tag{42}
$$

$$
\begin{aligned}
\dot{y}_{i\gamma\sigma\theta} = & -\alpha_y Y_{i\gamma\sigma\theta} \\
& + g_x(X_{i\gamma\sigma\theta}) \\
& + \sum_{j \neq i, \gamma'\sigma'\theta'} W_{[i\gamma\sigma\theta, j\gamma'\sigma'\theta']} g_x(x_{j\gamma'\sigma'\theta'}) \\
& + I_c
\end{aligned}
\tag{43}
$$

where $\alpha_x x_{i\gamma\sigma\theta}$ and $\alpha_y Y_{i\gamma\sigma\theta}$ model the decay to the resting potential, $g_x(x)$ and $g_y(y)$ are sigmoid-like functions modeling cells' firing rates in response to membrane potentials x and y, respectively, $\Psi(\gamma', \Delta_\sigma, \Delta_\theta) \leq 1$ is the spread of inhibition within a hypercolumn, $J_0 g_x(x_{i\gamma\sigma\theta})$ is self-excitation, and I_c is background noise [7]. Any cell can interact with another by exciting it or inhibiting it, via monosynaptic excitation through excitatory-excitatory horizontal connections, or disynaptic inhibition through excitatory-inhibitory connections, respectively [9]. Such interactions are modeled between cells within and across hypercolumns; color, scale, and orientation, as well as between cells within and across cell classes; double-opponent and single-opponent. These cellular interactions are defined by $J_{[i\gamma\sigma\theta, j\gamma'\sigma'\theta']}$ (excitatory) and $W_{[i\gamma\sigma\theta, j\gamma'\sigma'\theta']}$ (inhibitory).

Orientation (θ): The excitatory and inhibitory interactions between orientation specific double-opponent cells are exactly as those defined by Penacchio [9] and Li [7]. Single-opponent cells, introduced in our work, are non-directional; they have no preferred orientation θ. $\Delta\theta$ is thus not computable and so this class of cells do not *inhibit* the activity of other cells. Single-opponent cells do not contribute to W. In order to explore 'fill in' effects, however, we support parameterization of *excitatory* weights to and from single-opponent and double-opponent cells. This weight functions as $\Delta\theta$ and is equal for all preferred orientations of the double-opponent cells. These interactions are modeled by a circular-symmetric gaussian in J.

Scale (σ): As in Penacchio [9], we decompose the input signal into signal at different scales. This reflect single-opponent and double-opponent cells' spatial frequency selectivity derived from their receptive fields. While this confers a level of scale invariance to the model, the primate visual cortex is not completely scale invariant and nor should our model be. Both image transformation methods presented in Stage I inherently represent activity at lower spatial frequencies with higher response.

Color (γ): We introduce a novel concept to the neurodynamical model framework developed by Li [7] and Penacchio [9]: color. Unfortunately, the structural organization of color preferring cells and the connections between them is not well understood and leading theories are still quite controversial [13]. We herein define a set of *logical* rules of interaction opponent color cells (including achromatic cells).

If a cell is stimulated, it excites nearby cells of the same orientation and scale preference, in any color channel other than its opponent. Conversely, a stimulated cell will inhibit nearby cells of the same orientation and scale preference, only in its opponent color channel. For example, stimulation of a DO cell preferring 'yellow' vertical edges will excite a DO cell preferring 'red' vertical edges at the same location. It will equally excite 'green', 'light', and 'dark' cells preferring the same orientation in the same location. It will not, however, excite cells of its opponent color 'blue'. In fact, it will inhibit activity in 'blue' cells preferring this same orientation in the same location.

We propose that these rules of interaction are logical as only opponent colors are mutually exclusive. While a bluish yellow line is not permissible in the opponent colorspace, a bluish green, bluish red, bright blue, or dark blue line is entirely plausible. Each of the possible combinations are equally probable and so the excitatory-excitatory connections between cells of these color preferences are equally weighed. These excitatory and inhibitory rules are encoded in J and W, respectively.

Activity Normalization (I_0): The general and local normalization of activities [**?**] has been extended from its used by Li [7] and Penacchio [9]. We normalize excitatory membrane potentials within double-opponent cells of similar location (i), color (γ), scale (σ), and orientation (θ) preferences. Likewise we normalize single-opponent cells of similar location (i), color (γ), scale (σ). We found it important to normalize the activity of these two classes of neurons independently as the information encoded by each is radically different: localized edge information by double-opponent cells, and extensive surface information by single-opponent cells.
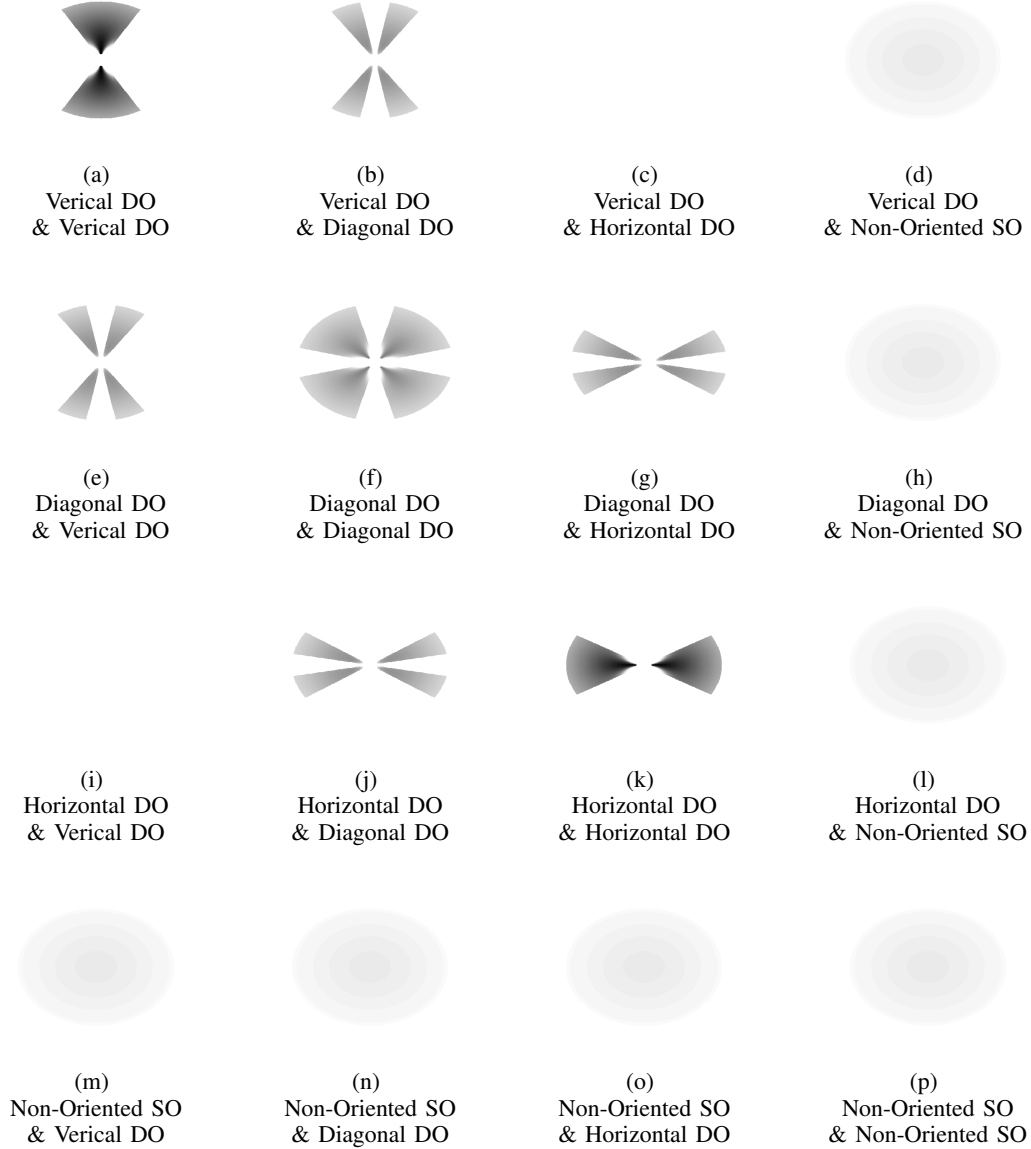

(a)
Verical DO
& Verical DO

(b)
Verical DO
& Diagonal DO

(c)
Verical DO
& Horizontal DO

(d)
Verical DO
& Non-Oriented SO

(e)
Diagonal DO
& Verical DO

(f)
Diagonal DO
& Diagonal DO

(g)
Diagonal DO
& Horizontal DO

(h)
Diagonal DO
& Non-Oriented SO

(i)
Horizontal DO
& Verical DO

(j)
Horizontal DO
& Diagonal DO

(k)
Horizontal DO
& Horizontal DO

(l)
Horizontal DO
& Non-Oriented SO

(m)
Non-Oriented SO
& Verical DO

(n)
Non-Oriented SO
& Diagonal DO

(o)
Non-Oriented SO
& Horizontal DO

(p)
Non-Oriented SO
& Non-Oriented SO

Fig. 12: Graphical representation of *excitatory* interaction weights (J) between vertical, diagonal, and horizontal double-opponent cells and single-opponent cells.
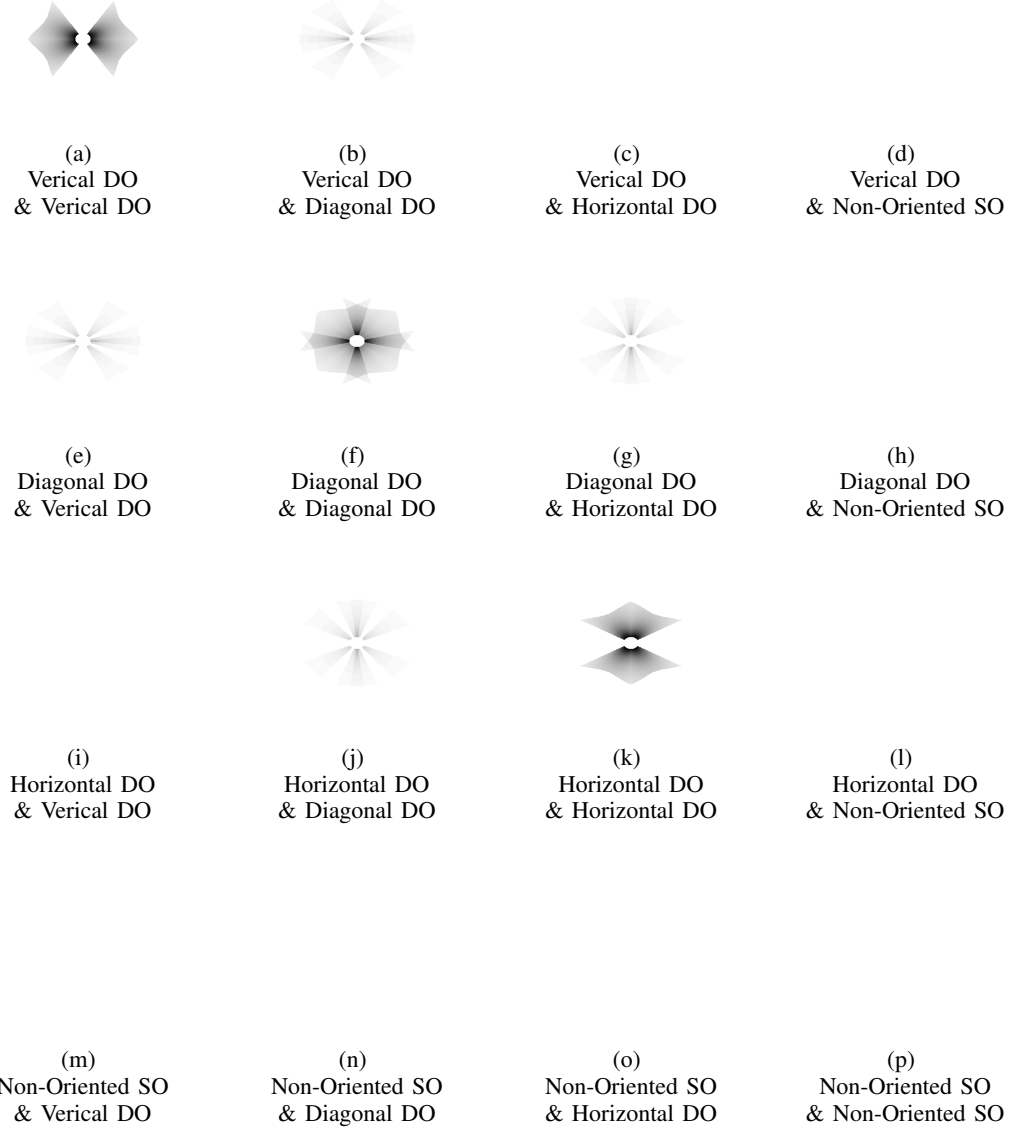
(a) Verical DO & Verical DO	(b) Verical DO & Diagonal DO	(c) Verical DO & Horizontal DO	(d) Verical DO & Non-Oriented SO
(e) Diagonal DO & Verical DO	(f) Diagonal DO & Diagonal DO	(g) Diagonal DO & Horizontal DO	(h) Diagonal DO & Non-Oriented SO
(i) Horizontal DO & Verical DO	(j) Horizontal DO & Diagonal DO	(k) Horizontal DO & Horizontal DO	(l) Horizontal DO & Non-Oriented SO
(m) Non-Oriented SO & Verical DO	(n) Non-Oriented SO & Diagonal DO	(o) Non-Oriented SO & Horizontal DO	(p) Non-Oriented SO & Non-Oriented SO

Fig. 13: Graphical representation of *inhibitory* interaction weights (W) between vertical, diagonal, and horizontal double-opponent cells and single-opponent cells.

IV. EXPERIMENTS

We evaluated the performance of our model by applying it to a number of test images seen to exhibit color induction effects. The expectation was that the model predict the perceived phenomena.

All experiments involved two or more test stimuli in which human observers can describe a difference between them. For example, most would describe the left inner ring in Figure **??** as being green and the right inner ring as being blue. As is shown, however, the two rings are physically identical; they have the exact same pixel values.

All test images were paired such that the effects caused two physically similar regions to appear to be different colors. The output of the model was the retinotopic neural activity in each of the opponent channels. For each pair of test patches, we compared the activity to 1) identify differences in activity and 2) to observe differences in the *direction* of activity. For example, in Figure **??** we expect to see neural activity to the left inner circle move toward green on the red-green axis, and the right inner circle move toward blue on the blue-yellow axis. Because the unit of neuronal activity is arbitrary, it cannot be used to generate a color image of what the model predicts, a so called 'perceptual image'. However, the unit is self-consistent and so can be compared between stimuli to evaluate magnitude and direction of activity.

//TODO *REWORK THIS PARAGRAPH.. IT'S NOT GREAT*

The perceived color is defined by the true color of the ring, the color(s) of the surrounding ring(s), and the interaction between them all.

Analyze Data Transformation

- Opponent Receptive Fields
  - does SO behave as expected
  - does DO behave as expected
  - does Itti space behave as expected
- DWT
  - does SO behave as expected (as Itti?)
  - does DO behave as expected
  - (L*a*b* is trusted)
- What are the differences between these outputs?
  - Show side by side LDRGBY/LAB+- convolutions
- What are general shortcomings?
  - OFF receptive fields function in time: removing green excites red. Our RFs don't reflect this.

Analyze Neurodynamical Model

- We can trust the concept because of Otazu 2013
- We need to analyze how color works
  - Connections between color channels
    * What are our assumptions? (& why?)
    * How does it modify the results over no connections?
    * How does it modify the results over full connections (including between opponents)?
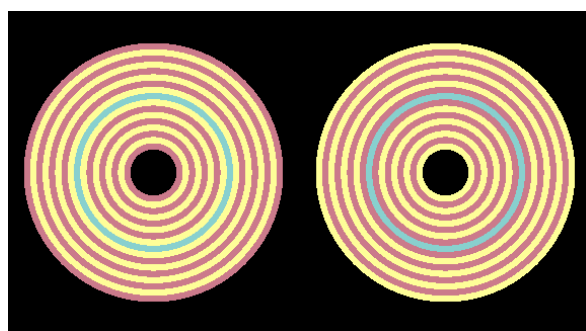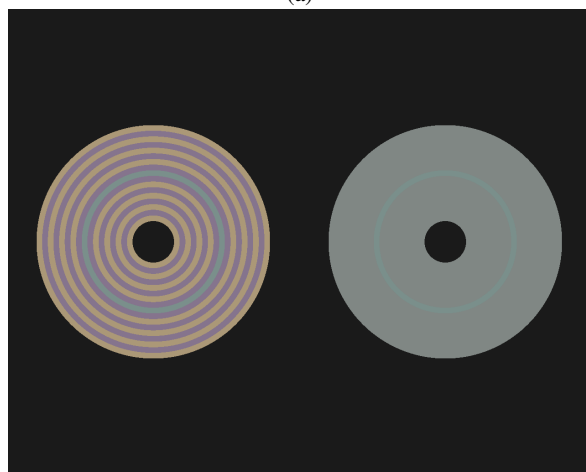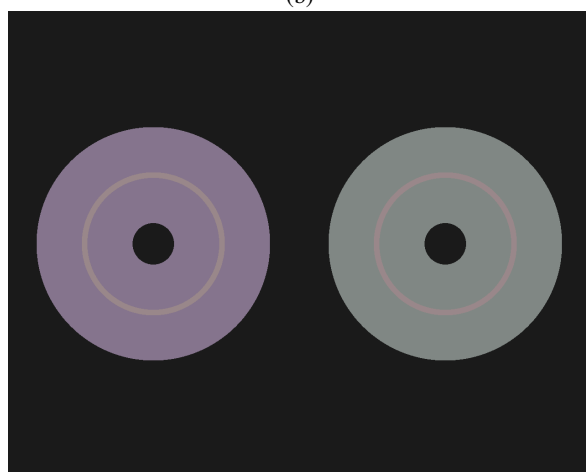 - Connections between SO and DO

V. RESULTS
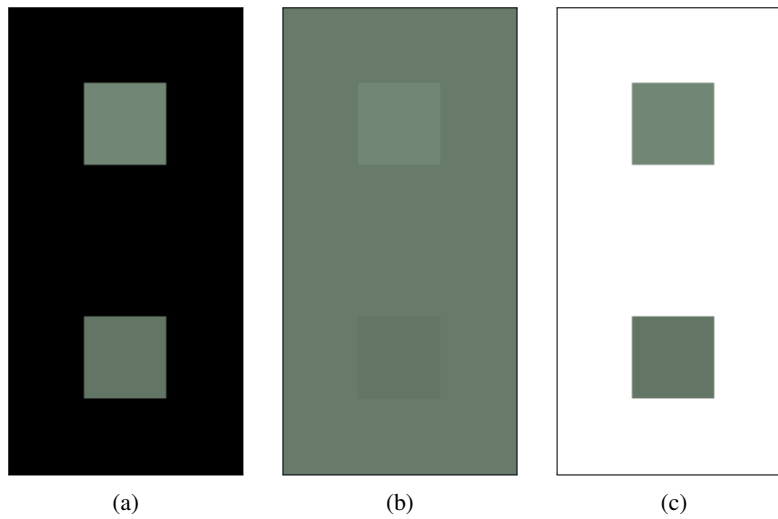
Fig. 14: Example of the 'Crispening Effect'; the lightness contrast between two patches becomes most significant when placed on a background whose luminance lies between those of the patches.
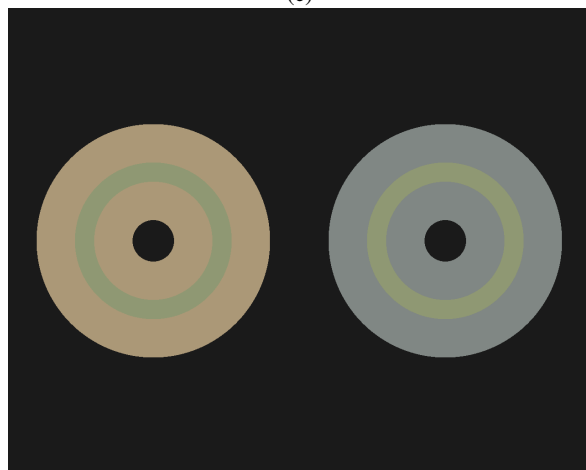
(a)

(b)

(c)

(d)

Fig. 15: Test images used to evaluate performance. In each image, the inner ring on the left is the exact same physical color (same pixel values) as the inner ring on the right.

(a)

(b) Light Dark   (c) Light Dark   (d) Light Dark   (e) Light Dark

(f) Red Green   (g) Red Green   (h) Red Green   (i) Red Green

(j) Blue Yellow   (k) Blue Yellow   (l) Blue Yellow   (m) Blue Yellow
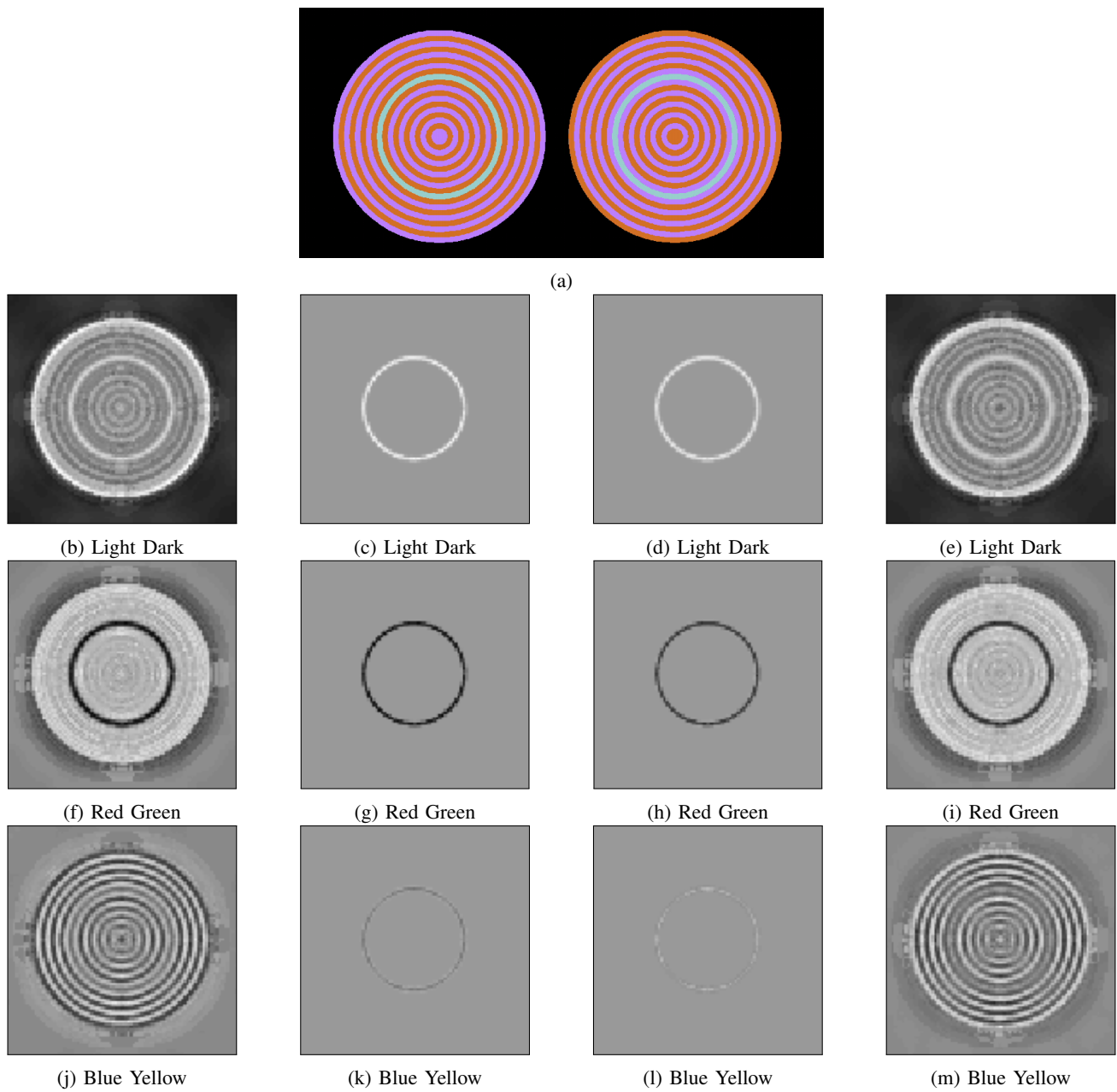
Fig. 16: Experimental results for the given test stimuli, 16a. In 16b, 16f, and 16j we have the raw output of the L-D, R-G, and B-Y channels for the *left* stimulus (which appears green). In 16e, 16i, and 16m we have the raw output of the L-D, R-G, and B-Y channels for the *right* stimulus (which appears blue). In 16c, 16g, and 16k we mask the raw output of the *left* stimulus so as to isolate the test ring. In 16d, 16h, and 16l we mask the raw output of the *left* stimulus so as to isolate the test ring.

(a)

(b) Light Dark (c) Light Dark (d) Light Dark (e) Light Dark

(f) Red Green (g) Red Green (h) Red Green (i) Red Green

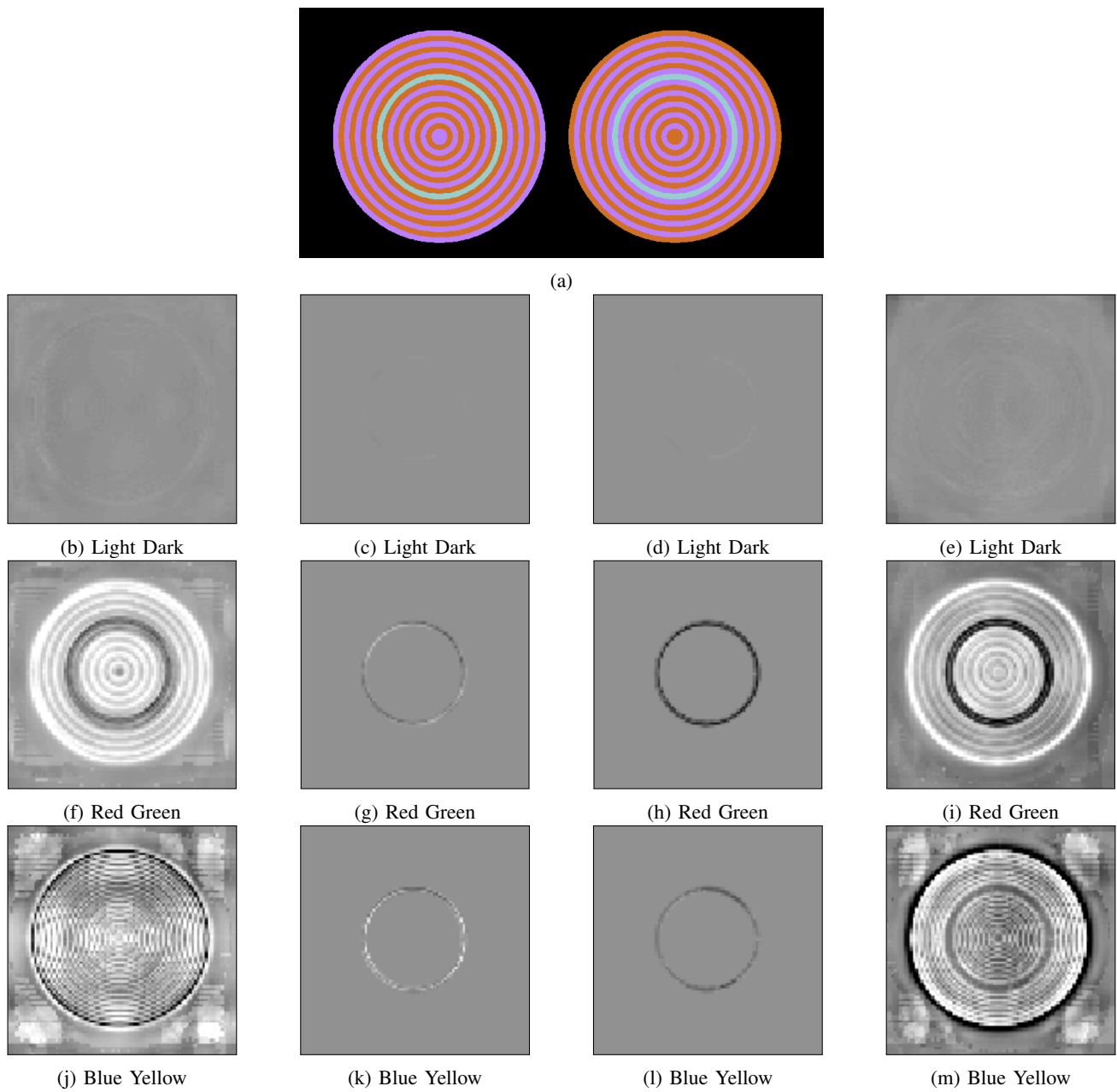(j) Blue Yellow (k) Blue Yellow (l) Blue Yellow (m) Blue Yellow

Fig. 17: Experimental results for the given test stimuli, 17a. In 17b, 17f, and 17j we have the raw output of the L-D, R-G, and B-Y channels for the *left* stimulus (which appears green). In 17e, 17i, and 17m we have the raw output of the L-D, R-G, and B-Y channels for the *right* stimulus (which appears blue). In 17c, 17g, and 17k we mask the raw output of the *left* stimulus so as to isolate the test ring. In 17d, 17h, and 17l we mask the raw output of the *left* stimulus so as to isolate the test ring.

(a)

(b) Light Dark

(c) Light Dark

(d) Light Dark

(e) Light Dark

(f) Red Green

(g) Red Green

(h) Red Green

(i) Red Green

(j) Blue Yellow

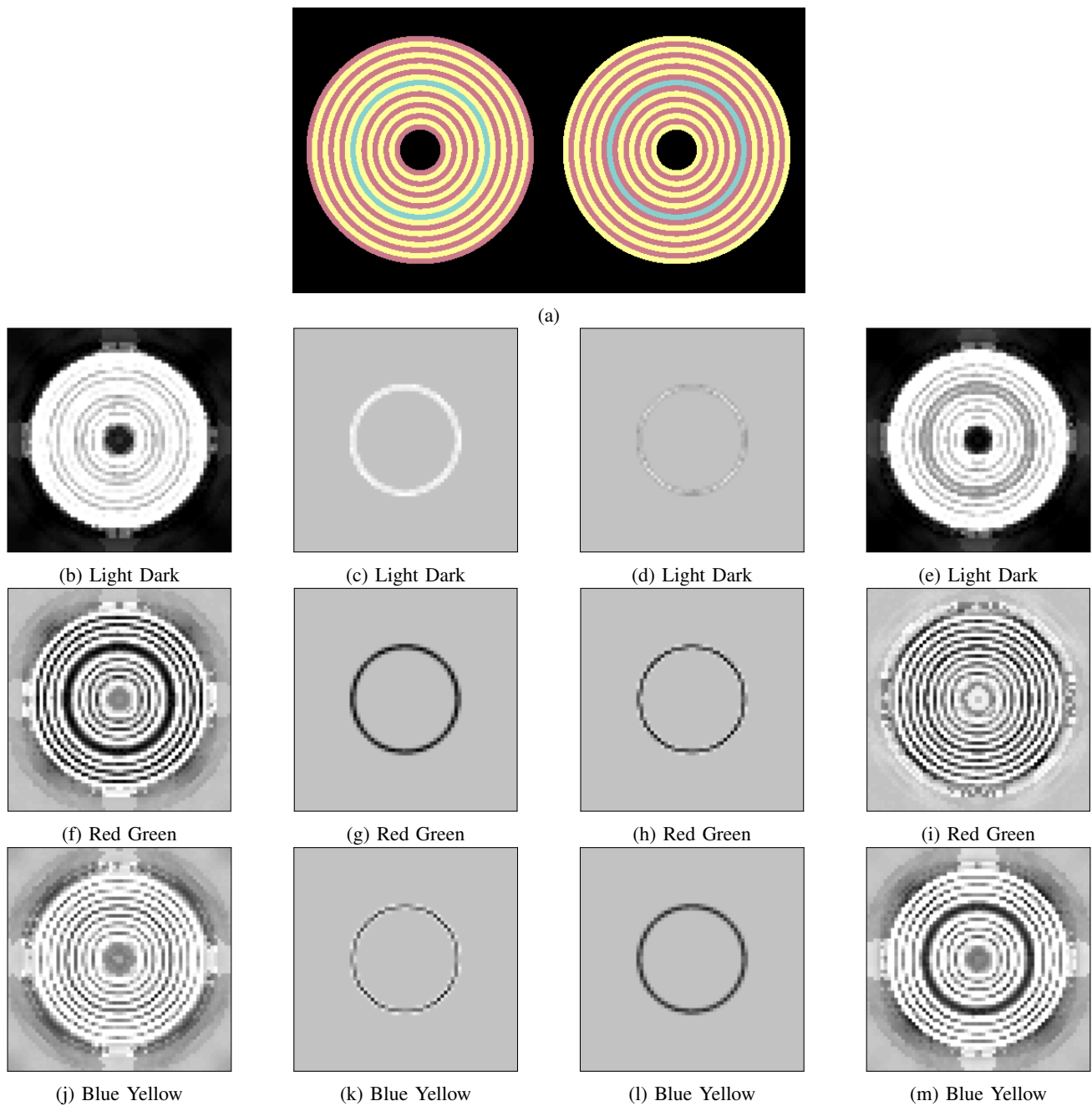(k) Blue Yellow

(l) Blue Yellow

(m) Blue Yellow

Fig. 18: Experimental results for the given test stimuli, 18a. In 18b, 18f, and 18j we have the raw output of the L-D, R-G, and B-Y channels for the *left* stimulus (which appears green). In 18e, 18i, and 18m we have the raw output of the L-D, R-G, and B-Y channels for the *right* stimulus (which appears blue). In 18c, 18g, and 18k we mask the raw output of the *left* stimulus so as to isolate the test ring. In 18d, 18h, and 18l we mask the raw output of the *left* stimulus so as to isolate the test ring.

(a)

(b) Light Dark   (c) Light Dark   (d) Light Dark   (e) Light Dark

(f) Red Green   (g) Red Green   (h) Red Green   (i) Red Green

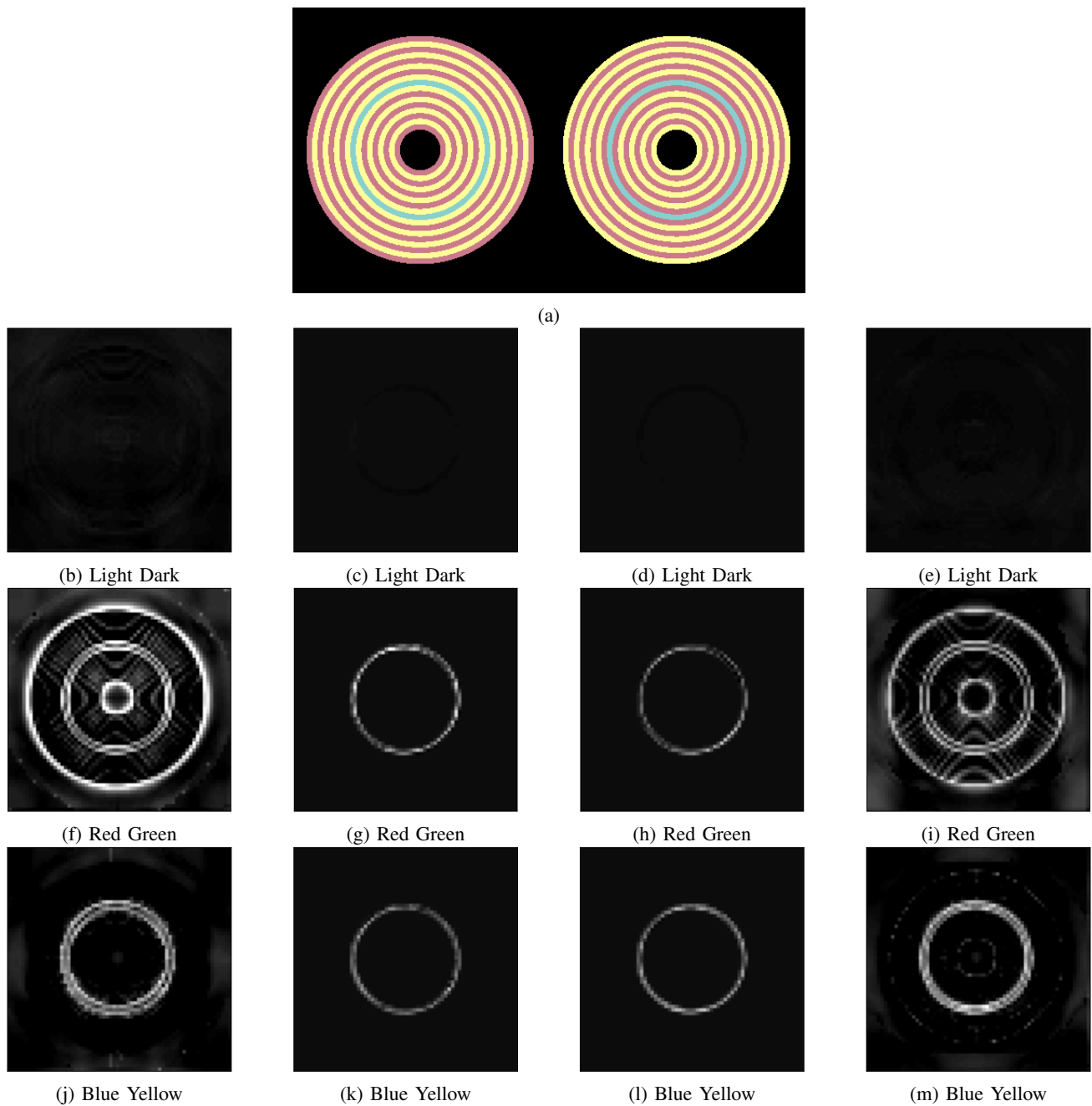(j) Blue Yellow   (k) Blue Yellow   (l) Blue Yellow   (m) Blue Yellow

Fig. 19: Experimental results for the given test stimuli, 19a. In 19b, 19f, and 19j we have the raw output of the L-D, R-G, and B-Y channels for the *left* stimulus (which appears green). In 19e, 19i, and 19m we have the raw output of the L-D, R-G, and B-Y channels for the *right* stimulus (which appears blue). In 19c, 19g, and 19k we mask the raw output of the *left* stimulus so as to isolate the test ring. In 19d, 19h, and 19l we mask the raw output of the *left* stimulus so as to isolate the test ring.
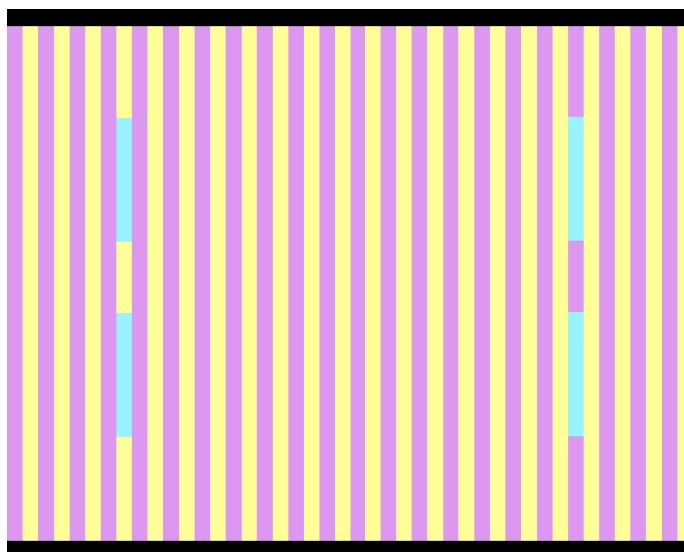
Fig. 20: Test image used to evaluate performance. The two bars on the left are the exact same physical color (same pixel values) as those on the right.

VI. CONCLUSIONS

References

[1] Conway, B. R., S. Chatterjee, G. D. Field, G. D. Horwitz, E. N. Johnson, K. Koida, and K. Mancuso. *Advances in Color Science: From Retina to Behavior*. Journal of Neuroscience 30.45 (2010): 14955-4963.

[2] Heeger, D. *Modeling simple-cell direction selectivity with normalized, half-squared, linear operators* Neurophysiology 70.5 (1993): 1885-1898.

[3] Itti L., Koch C., and Niebur E. *A Model of Saliency-Based Visual Attention for Rapid Scene Analysis*. IEEE Transactions on Pattern Analysis and Machine Intelligence, 20.11 (1999). 1254-1259.

[4] Johnson, E., Hawken, M., and Shapley, R. *The Orientation Selectivity of Color-Responsive Neurons in Macaque V1*. Journal of Neuroscience 28.32 (2008): 8096-106

[5] Lennie, P., Haake, W., and Williams, D. *Color in the Primary Visual Cortex*. Computational Models of Visual Processing. Cambridge, Mass.: MIT, (1991): 71-82.

[6] Zhaoping Li. *A Neural Model of Contour Integration in the Primary Visual Cortex*. Neural Computation 10.4 (1998): 903-40.

[7] Zhaoping Li. *Visual Segmentation by Contextual Influences via Intra-cortical Interactions in the Primary Visual Cortex*. Network: Computation in Neural Systems 10.2 (1999): 187-212.

[8] Otazu, X., Parraga, C., and Vanrell, M. *Toward a Unified Chromatic Induction Model*. Journal of Vision 10.12 (2010): 5.

[9] Penacchio O., Otazu, X., and Dempere-Marco, L. *A Neurodynamical Model of Brightness Induction in V1*. PLoS ONE 8.5 (2013): E64086.

[10] Ramirez-Villegas, J., and Ramirez-Moreno, D. *Color Coding in the Cortex: A Modified Approach to Bottom-up Visual Attention*. Biological Cybernetics 107.1 (2013): 39-47.

[11] Robert, S., Hawken, M., and Johnson, E. *Color in the Primary Visual Cortex*. The Visual Neurosciences. Vol. 2. Cambridge, Mass.: MIT, (2004): 568-86.

[12] Schluppeck, D., and S. A. Engel. *Color Opponent Neurons in V1: A Review and Model Reconciling Results from Imaging and Single-Unit Recording*. Journal of Vision 2.6 (2002): 480-492.

[13] Shapley R. and Hawken M. *Color in the Cortex: Single- and Double-opponent Cells*. Vision Research 51.7 (2011): 701-17.

[14] Sincich, Lawrence C., and Jonathan C. Horton. *THE CIRCUITRY OF V1 AND V2: Integration of Color, Form, and Motion*. Annual Review of Neuroscience 28.1 (2005): 303-26.

[15] Solomon, Samuel G., and Peter Lennie. *The Machinery of Colour Vision*. Nature Reviews Neuroscience 8.4 (2007): 276-86.

[16] Hedva Spitzer, Yuval Barkan. *Computational adaptation model and its predictions for color induction of first and second orders*. Vision Research 45.27 (2005). 33233342.

[17] Yang K., Gao S., Li C, and Li Y. *Efficient Color Boundary Detection with Color-opoonent Mechanisms*. Computer Vision and Pattern Recognition (CVPR), (2013), pp 2810-2817.

[18] Jun Zhang, Youssef Barhomi, and Thomas Serre. *A new biologically inspired color image descriptor*. Computer Vision ECCV 2012 Lecture Notes in Computer Science Volume 7576, (2012): 312-324.